Scientific Research Publishing

Advances in Materials Physics and Chemistry, 2026, 16(5), 161-175
https://www.scirp.org/journal/ampc
ISSN Online: 2162-5328
ISSN Print: 2162-531X

# Enhancing Strategy of CIGS-Based Thin-Film Solar Cells Performances by Optimizing the Transparent Conductive Oxide (TCO) Layer

**Adama Zongo, Soumaïla Ouédraogo, Boureima Traoré, Issiaka Sankara, Marcel Bawindsom Kébré, François Zougmoré, Zacharie Koalga, Frédéric Ouattara**

Laboratoire de Matériaux et Environnement (LA.M.E)-UFR/SEA, Université Joseph Ki-Zerbo, Ouagadougou, Burkina Faso
Email: zongamss@gmail.com

**How to cite this paper:** Zongo, A., Ouédraogo, S., Traoré, B., Sankara, I., Kébré, M.B., Zougmoré, F., Koalga, Z. and Ouattara, F. (2026) Enhancing Strategy of CIGS-Based Thin-Film Solar Cells Performances by Optimizing the Transparent Conductive Oxide (TCO) Layer. *Advances in Materials Physics and Chemistry*, **16**, 161-175.
https://doi.org/10.4236/ampc.2026.165008

**Received:** February 3, 2026
**Accepted:** May 23, 2026
**Published:** May 26, 2026



## Abstract

In this paper, based on numerical simulation, we use SCAPS-1D software to analyze the electrical and optical properties of the transparent conductive oxide (TCO) layer and the interface between the TCO layer and the CdS buffer layer on the performance of the CIGS solar cell. To achieve our purpose, we studied the important parameters of the TCO layer, such as its thickness and doping. For the TCO/CdS interface, we analyzed the impact of the conduction band offset (CBO) due to the band alignment. Numerical simulation results show that the thickness and doping of the TCO layer are crucial parameters for optimizing the electrical and optical parameters of CIGS-based solar cells. The optimal values for the electrical (open-circuit voltage, current density, fill factor and efficiency) and optical (quantum efficiency) parameters are obtained when the TCO layer thickness is in the range 0.025 and 0.035 μm, and the doping in the order of $10^{15}$ $cm^{-3}$. The study of band alignment at the TCO/CdS interface has shown that strong negative conduction band offset (cliff) or strong positive conduction band offset (peak) favors recombination at this interface. Very good performances are obtained for a conduction band offset at the CdS/ZnO interface of no more than −0.3 eV (CBO(CdS/ZnO) ≈ −0.3 eV).

## Keywords

Numerical Simulation, CdS/TCO Interface, Interface Defects, Conduction Band Offset, Transparent Conductive Oxide

## 1. Introduction

CIGS technology thin-film solar cells represent a high hope for the future of PV,

because of their low production costs and excellent conversion efficiencies, which are close to those of crystalline silicon solar cells [1]. Improving the performance of the CIGS-based PV solar cell has been the subject of several publications. It has been very successful and now tends to rival silicon-based solar cells, which account for around 80% of the world market. The thin-film solar cell based on CIGS is made up of several layers but the one that will attract our attention is the transparent conductive oxide (TCO) layer. Other TCO proposed by various laboratories, such as indium tin oxide (ITO), fluorine-doped tin oxide ($SnO_2$:F), zinc sulphide (ZnS), zinc selenide (ZnSe) and many others, can offer interesting electrical and optical performances. Several research projects have led to the outstanding properties of zinc oxide (ZnO), which is used as a window layer. ZnO is recognized as the most suitable TCO, which has increased the efficiency of the CIGS/CdS/ZnO solar cell, making it one of the most efficient. This discovery is encountering difficulties linked to ZnO deposition techniques, which require huge amounts of energy, and efforts must be made to find solutions. Several deposition techniques such as sputtering, chemical vapor deposition and electrochemical deposition are used to obtain a suitable window layer. A thin CdS buffer layer is used to passivate the surface of the CIGS layer to mitigate the degradation of the CIGS layer by the high energy ZnO deposition. However, despite all these efforts, the CdS/ZnO interface is seen as a recombination zone for charge carriers [2]-[4]. To minimize the recombination phenomen at this interface, these optimization techniques such as layer growth control, heat treatment, controlled doping and surface cleaning can be used [5]-[7]. In-depth characterization and modelling studies can help to understand the underlying mechanisms of defects at the CdS/ZnO interface and propose solutions to improve the performance of CIGS-based solar cells. Many factors linked to the physico-chemical aspect of the ZnO layer can contribute to the reduction in light transmission and the transport of charge carriers. Optimizing the thickness of the ZnO layer improves the transmission of sunlight and the quality of its contact with the CdS layer. Crystallographic defects in the grain boundaries at the CdS/ZnO interface can favour the recombination of charge carriers that contribute to the creation of the solar cell's output current density. In this paper, we have studied the influence of the window layer properties (thickness and doping) on the electrical parameters of the solar cell. An analysis of the ZnO/CdS interface through conduction band alignment was carried out. The results obtained show that the properties of the ZnO layer and the conduction band offset at the ZnO/CdS interface are crucial for obtaining a CIGS cell with high conversion efficiency.

## 2. Device Model and Simulation Details

We used the most recent version of SCAPS-1D software to carry out the numerical simulations [8]-[10]. The structure of the solar cell is made up of five layers deposited one on top of the other. All these layers are deposited on a metallic soda-lime glass substrate. The copper indium gallium diselenide (CIGS) absorber is de-

posited by sputtering and represents the active layer of the solar cell. A thin $MoSe_2$ layer forms at the interface between the CIGS absorber and the molybdenum (Mo) back contact, which can be considered a defect. A thin cadmium sulfide (CdS) layer between 50 and 80 nm thick, is usually deposited on the CIGS absorber by chemical bath deposition (CBD). The cadmium (Cd) contained in the CdS buffer layer diffuses into the surface regions of the absorber to form a thin surface defect layer (SDL) at the CdS/CIGS interface [11] [12]. One of the fundamental roles of the N-type conductivity CdS buffer layer is to form the P-N heterojunction with the P-type conductivity CIGS absorber. Finally, a transparent conductive layer (TCO) consisting of zinc oxide (ZnO) is deposited on the CdS as an anti-reflective layer for light rays and also to protect the cell. This layer (TCO) has two major qualities. It must be transparent and sufficiently conductive. It is usually deposited by sputtering. This window layer consists of two layers, a thin layer of intrinsic zinc oxide (i-ZnO) and a thick layer of aluminum-doped zinc oxide (ZnO:Al). The ZnO conductive layer is frequently doped with aluminum (ZnO:Al), but other dopants such as boron (ZnO:B) [13] or gallium (ZnO:Ga) [14] also exist.

A nickel/aluminum (Ni/Al) metal grid crowns the solar cell and represents the ohmic contact. It enables electrons to be collected efficiently and transferred to an external circuit. The structure of such a solar cell is shown in **Figure 1**.

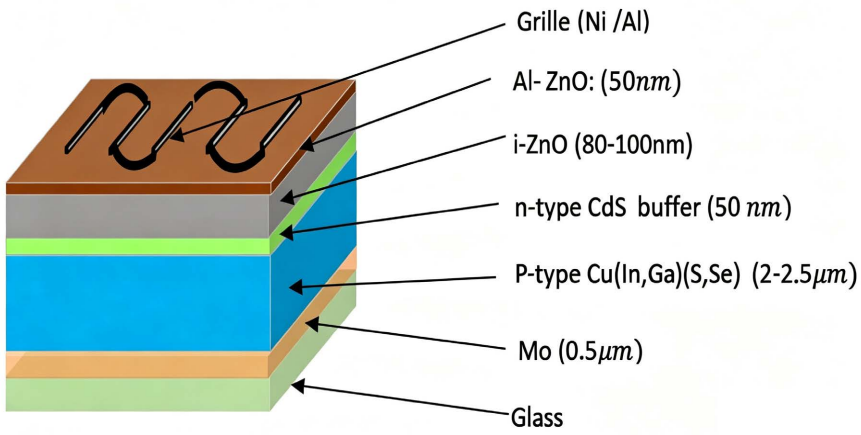


**Figure 1.** Structure of CIGS solar cell.

To study the optoelectrical properties of the various parameters of our model, we used the SCAPS-1D (Solar Cell Capacitance Simulator 1 dimension) software. SCAPS-1D is a software package developed at the University of Ghent in Belgium in the Electronics end Informatics Systems (ELIS) Department. One of the reasons for its use is its ability to simulate heterojunction solar cells with up to seven layers in addition to front and back contacts [15]. The simulation with SCAPS-1D is based on the resolution of the electron continuity Equation (1) and hole continuity Equation (2) and Poisson Equation (3), which are fundamental in the characterization of photovoltaic solar cells. The continuity equations describe the variation per unit time in the number of charge carriers and determine the different

currents in a semiconductor, while Poisson's equation is used to determine the electrostatic potential associated with a charge distribution $\rho$.

$$\begin{cases} \dfrac{\mathrm{d}p}{\mathrm{d}t} = \dfrac{1}{q} \cdot \dfrac{\mathrm{d}J_P}{\mathrm{d}x} + r_p - g_p & (1) \\ \dfrac{\mathrm{d}n}{\mathrm{d}t} = \dfrac{1}{q} \cdot \dfrac{\mathrm{d}J_n}{\mathrm{d}x} - r_n + g_n & (2) \end{cases}$$

With $r_n$ ($r_p$) the electron (hole) recombination rate, $g_n$ ($g_p$) the electron (hole) generation rate as a function of depth $x$, and $\vec{j}_n$ ($\vec{j}_p$) the electron (hole) current density.

$$\frac{d^2\psi}{x^2} = \frac{\rho}{\varepsilon_r \varepsilon_0} \quad (3)$$

With $\psi$ the electrostatic potential, $\rho$ the space charge and $\varepsilon_0$ and $\varepsilon_r$ the vacuum and relative dielectric constants respectively.

**Table 1.** Basic parameters of the different layers of solar cell [6].

| Cell general propeties | Front cantact | | Back contact |
|---|---|---|---|
| $\phi_b(\mathrm{eV})$ | $\phi_{b_n} = 0$ | | $\phi_{b_p} = 0.2$ |
| $S_e(\mathrm{cm/s})$ | $10^7$ | | $10^7$ |
| $S_h(\mathrm{cm/s})$ | $10^7$ | | $10^7$ |
| *Reflectivity* | 0.05 | | 0 |
| **Layer properties** | **ZnO** | **CdS** | **$CuInGaSe_2$** |
| $W(\mathrm{nm})$ | 70 | 50 | 3000 |
| $\varepsilon/\varepsilon_0$ | 9 | 10 | 13.6 |
| $\mu_e(\mathrm{cm^2/s})$ | 100 | 100 | 100 |
| $\mu_h(\mathrm{cm^2/s})$ | 25 | 25 | 25 |
| $N_{A/D}(\mathrm{cm^{-3}})$ | $N_D = 10^{18}$ | $N_D = 1.1\times10^{18}$ | $N_A = 2\times10^{16}$ |
| $E_g(\mathrm{eV})$ | 3.3 | 2.4 | 1.15 |
| $N_c(\mathrm{cm^{-3}})$ | $2.2 \times 10^{18}$ | $2.2 \times 10^{18}$ | $2.2 \times 10^{18}$ |
| $N_v(\mathrm{cm^{-3}})$ | $1.8 \times 10^{19}$ | $1.8 \times 10^{19}$ | $1.8 \times 10^{19}$ |
| $\chi(\mathrm{eV})$ | 4.45 | 4.45 | 4.5 |
| **Gaussian-distributed defect states** | | | |
| $N_{A/D}(\mathrm{cm^{-3}})$ | $N_D = 10^{16}$ | $N_D = 5\times10^{16}$ | $N_A = 10^{14}$ |
| $W_G(\mathrm{eV})$ | 0.1 | 0.1 | 0.1 |
| $\sigma_e(\mathrm{cm^2})$ | $10^{-12}$ | $10^{-17}$ | $5 \times 10^{-13}$ |
| $\sigma_h(\mathrm{cm^2})$ | $10^{-15}$ | $10^{-12}$ | $10^{-15}$ |

The properties of the different layers, bulk and interface defects used for the numerical simulation are presented in Table 1. These properties are taken from

theoretical and experimental results (Gloeckler *et al.*, 2005) [16].

To validate our results, the J-V characteristic of our numerical model was compared with an experimental result from the literature [9]. There is good agreement between the simulated results and those obtained experimentally, thus validating our baseline parameters in Table 1.

The solar cell temperature is maintained at 300 K and is illuminated under standard conditions by an AM 1.5 G spectrum that accounts for both direct and diffuse radiation. In order to validate our results, we compared the J-V characteristic curves of our numerical simulation with that performed experimentally by Pettersson. A good agreement is found between these two results, as shown in Figure 2.

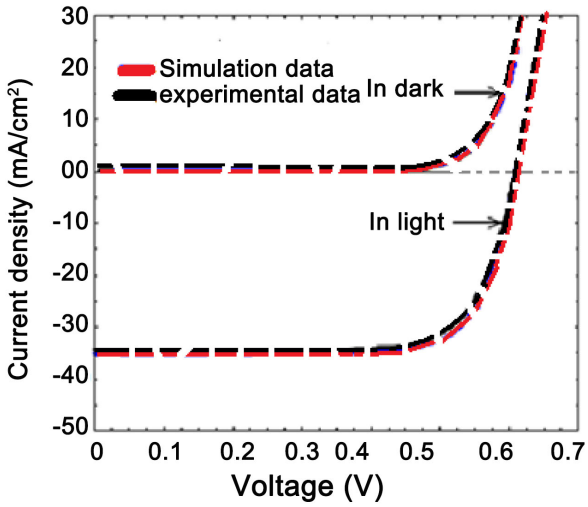


Figure 2. Comparison between the photocurrent density-voltage (J-V) curves for the simulated (red line) and the reported experimental data (black line).

## 3. Result and Discussion

### 3.1. Influence of Window Layer Thickness on Electrical and Optical Parameters

The thickness of the transparent conductive oxide (OTC) layer or window layer is an important parameter for optimizing solar cell performance.

The transparency and conductivity of this layer can be determined by its thickness. To improve the transparency and conductivity of the ZnO window layer, we studied the influence of its thickness. This study will consist of characterizing the performance of the solar cell on the current-voltage (J-V) characteristic and the quantum efficiency (QE). To carry out our numerical simulation, we varied the thickness of the ZnO layer from 0.01 μm to 0.1 μm with a step of 0.02 μm while fixing the thickness of the CIGS absorber at 2.8 μm and that of the CdS buffer layer at 0.05 μm. The obtained results are shown in Figure 3.

The absorption of incident photons decreases when the thickness of the window layer increases for short wavelengths. As shown in Figure 3(b). For long wavelength

photons, it can be seen that varying the thickness of the ZnO window layer in the solar cell slightly affects the (Q-E) characteristic. For a better interpretation of the (J-V) characteristic, we have extracted the electrical parameters of the solar cell. These electrical parameters as function of ZnO layer thickness are shown in Figure 4.

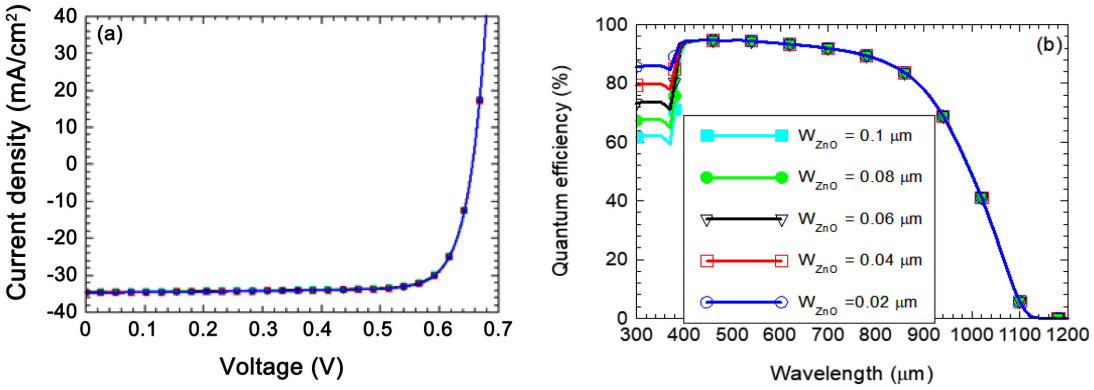


Figure 3. Effect of ZnO layer thickness on: (a) (J-V) Characteristic, (b) quantum efficiency (Q-E) of the solar cell.

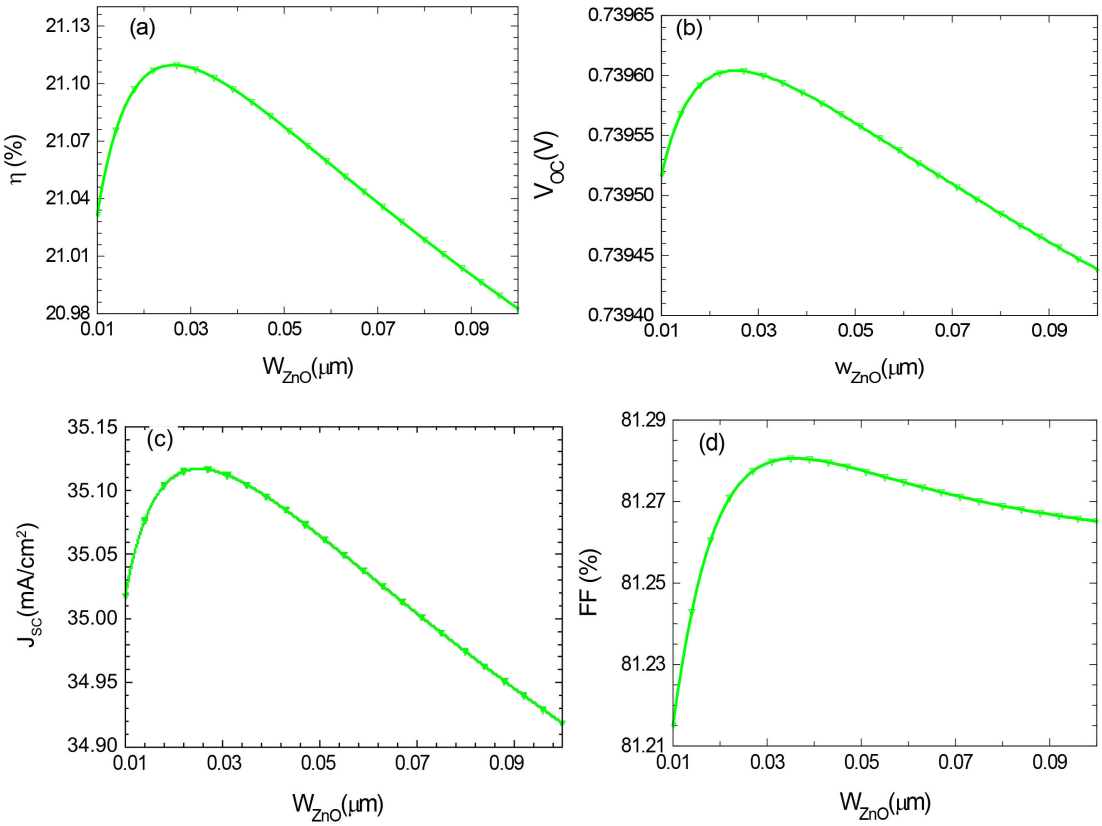


Figure 4. Evolution of the electrical parameters of the solar cell as a function of the thickness of the ZnO window layer.

All the electrical parameters of the solar cell increase when the window layer thicknesses ( $W_{ZnO} < 0.03$ µm). They are strongly degraded when the thickness of the ZnO layer becomes thick ( $W_{ZnO} > 0.03$ µm). These losses are explained by a reduc-

tion in the absorption of incident photons of short wavelength ($\lambda < 400$ nm), which prevents the transport of the photogenerated current at the PN junction. This loss is less marked with FF than with other electrical parameters.

Optimum solar cell performance is obtained for a window layer thickness between 0.025 and 0.035 µm. This allowed us to obtain, $\eta = 21.109\%$, $V_{OC} = 0.739604$ V, de $J_{SC} = 35.1169\ \mathrm{mA/cm^2}$ end FF = 81.2806%. In fact, the thickness of the ZnO layer must not exceed a certain value (0.02 µm < $W_{ZnO}$ < 0.04 µm), above 0.04 µm all the parameters degrade exponentially. This is justified by the equation for its transmission, which is inversely proportional to its absorption coefficient and thickness, given by Equation (4).

$$T = \mathrm{e}^{-\alpha W_{ZnO}} \tag{4}$$

where $T$ is the spectrum transmitted by the ZnO layer, $\alpha$ is the absorption coefficient and $W_{ZnO}$ is the ZnO layer thickness.

With increasing the ZnO layer thickness, the transmitted spectrum becomes weaker, reducing the number of incident photons reaching the active layer. It has also been shown that this layer, in conjunction with the buffer layer, reduces the local electrical losses associated with the non-uniformity of the absorber [17].

### 3.2. Influences of Window Layer Thickness and Doping

The charge carrier density within the ZnO layer significantly influences its optical properties and the electron efficiency at the metallic grid. The most commonly used element for doping ZnO is Group III (B, Al, Ga or In) or Group VII (Cl, Br or I) of the periodic table. For this study, aluminum (Al) was selected as dopant due to its positive effects on the CIGS solar cells, as reported in [11]-[14].

To evaluate the influence of this phenomenon, the thickness of the ZnO layer was varied from 0.01 µm to 0.1 µm for different donor densities from ($10^{13}$ $\mathrm{cm^{-3}}$ to $10^{17}$ $\mathrm{cm^{-3}}$), as shown in **Figure 5.** The analysis of the J-V characteristics and the quantum efficiency indicate that the appropriate doping level for optimal spectral utilization around $10^{14}$ $\mathrm{cm^{-3}}$.

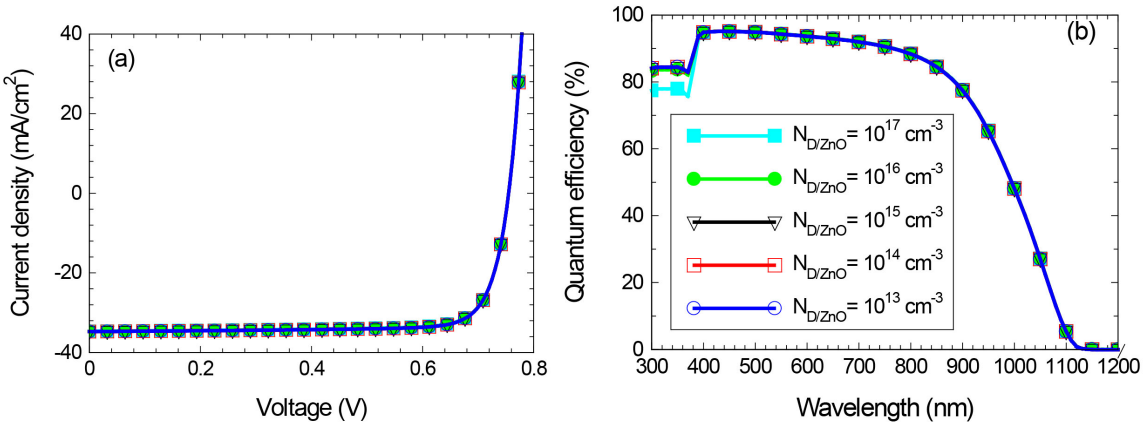


**Figure 5.** (a) Variation of the J-V characteristic and (b) quantum efficiency for different values of dopant densities in ZnO layer.

These results are further illustrated in **Figure 6**, which shows the behavior of the electrical parameters when the thickness and doping rate are varied. It is observed that efficiency, open-circuit voltage, and short-circuit of solar cell. A small quantity of aluminum-ratio impurities in the ZnO layer makes it possible to reduce the size of the grains, which constitute an electron recombination center [18]. In fact, ZnO can only transmit light at frequencies higher than its plasma frequency, which is proportional to the charge carrier density. With a high electron affinity (4.45 eV), the moderate current density and fill factor are improved as the doping density decreases. A maximum efficiency of 21.39% is obtained for $N_{D_{ZnO}} = 10^{15}\ \text{cm}^{-3}$ at $W_{ZnO} \approx 0.032\ \mu\text{m}$ and 81.61% for the fill factor for $N_{D_{ZnO}} = 10^{15}\ \text{cm}^{-3}$ at $W_{ZnO} \approx 0.038\ \mu\text{m}$. These parameters are strongly degraded at high densities ($10^{15}\ \text{cm}^{-3} < N_{D_{ZnO}}$) with a reduction of 0.075% in efficiency and 0.064% in FF. These results are in perfect agreement with the work of Duenow Joel N. *et al.* [18] who showed that the transmittance of (ZnO:Al) is influenced by the density of the dopants and the wavelengths of the solar spectrum. Increased doping enhances the bandgap, leading to absorption of a portion of the spectrum by the ZnO layer, which disrupts the optimal operation n-type doping of ZnO favors its conductivity. At high levels of doping, electron mobility in the semiconductor can be hindered by a number of phenomena. Mobility is associated to the propagation free time $\tau$ in Equation (5), collisions between electrons and dopant densities, defects in the material's crystal lattice, and also to vibrations created by phonons.

$$\mu = \frac{e\tau}{m^*} \tag{5}$$

With $e$ the electronic charge and $m^*$ the effective mass of the electron.

The analysis of bulk defect parameters has revealed that they can impede the correct performance of the cell if they are not controlled. In addition, surface defects act as charge carrier recombination centers, further reducing cell performance. In the rest of our work, we will study the impact of the contact between th e window layer and the buffer layer. The window layer is an overlay of a layer devoid of impurities denoted i-ZnO and a doped part denoted ZnO:Al. In this part, we evaluated the impact of the thickness of each part of the window layer on the cell performance. For different values of doping densities ($10^{15}$ $\text{cm}^{-3}$ to $10^{19}$ $\text{cm}^{-3}$), we have on the one hand, varied the thickness of the i-ZnO layer while keeping that of the ZnOAl at 0.02 μm. The results represented by **Figure 7**, also show that for the doping between $10^{15}$ $\text{cm}^{-3}$ and $10^{17}$ $\text{cm}^{-3}$, i-ZnO thickness affects the cell's electrical parameters, which decrease almost liberally with increasing i-ZnO thickness.

For low doping densities, the cell's electrical parameters decrease with increasing i-ZnO layer thickness, Conversely, for densities greater than $10^{17}$ $\text{cm}^{-3}$, we see an improvement in parameters with increasing thickness. The transparency of the ZnO layer therefore depends not only on the physical properties defined above but also on the dopant density. These results are in agreement with the research

of Abdelkader *et al.* [19], who showed that when the doping rate exceeds 8%, the conductivity of ZnO is reduced. In this case, aluminum no longer behaves as a doping element, but oxidizes in the presence of oxygen to form aluminum oxide $Al_2O_3$ which modifies the ZnO crystal lattice. Thus, a conversion efficiency of $\eta$ = 21.24% with a doping density of $10^{19}$ cm$^{-3}$ and $W_{i\text{-}ZnO}$ = 0.015 µm, and an efficiency of $\eta$ = 22.5% is obtained at $W_{i\text{-}ZnO}$ = 0.089 µm and $10^{19}$ cm$^{-3}$.

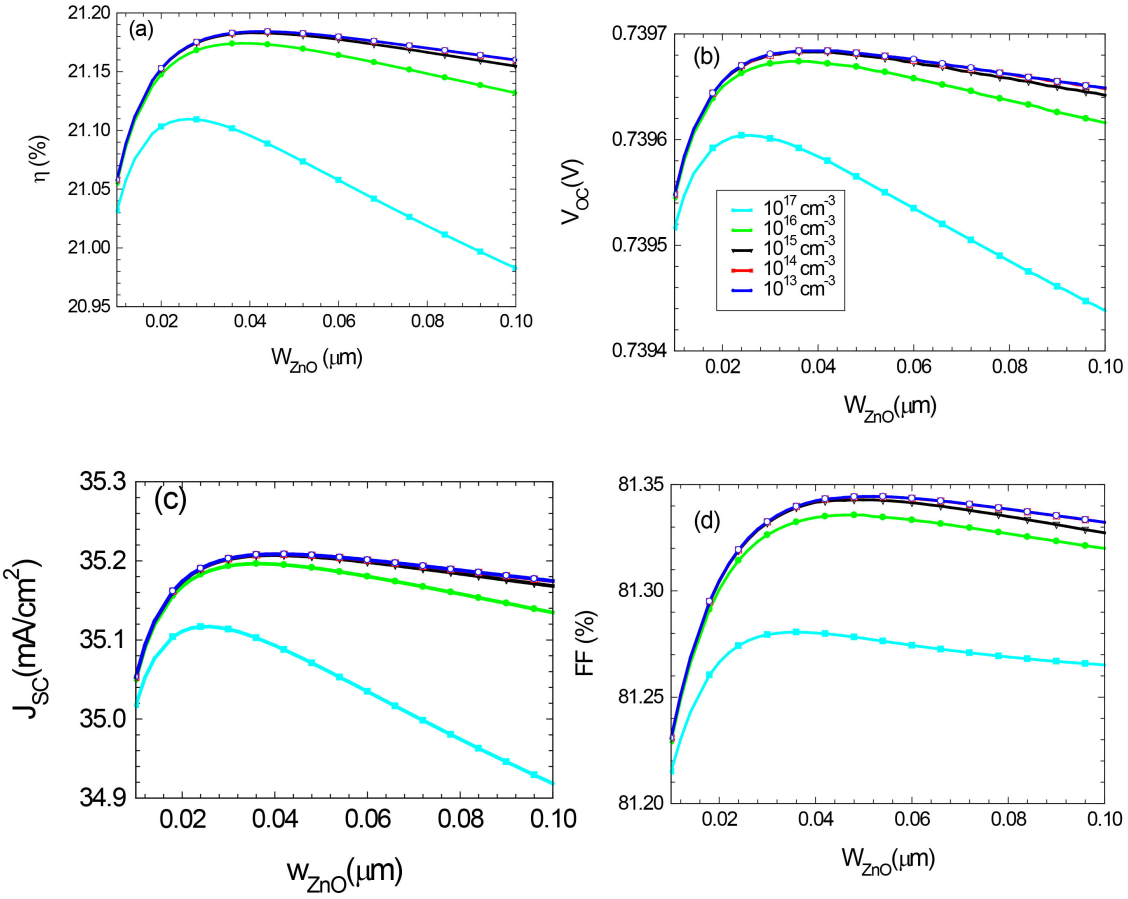


**Figure 6.** Variation of electrical parameters as a function of ZnO layer thickness for different dopant density values.

The best results of our simulation are obtained, when the i-ZnO layer thickness is greater than 0,07 µm with an open circuit voltage of 0.739 V at $W_{i\text{-}ZnO}$ = 0.082 µm and $N_D = 10^{19}$ cm$^{-3}$. A maximum form factor of 81.39% at $W_{i\text{-}ZnO}$ = 0.091 µm, and short-circuit current of 35.29 mA/cm$^2$ at $W_{i\text{-}ZnO}$ = 0.089 µm all at $N_D = 10^{19}$ cm$^{-3}$ are obtained. Increasing the thickness of the i-ZnO layer reduces the influence of interfacial defects and improves junction quality. It promotes better collection of photogenerated carriers and contributes to the stability of the fill factor. Studies have shown that the optimum thickness of an i-ZnO layers improves the stability and performance of the cell as a whole [20] [21]. On the other hand, we varied the thickness of the ZnO:Al layer and the density of defects in the same range as above while keeping that of the i-ZnO at 0.035 µm.

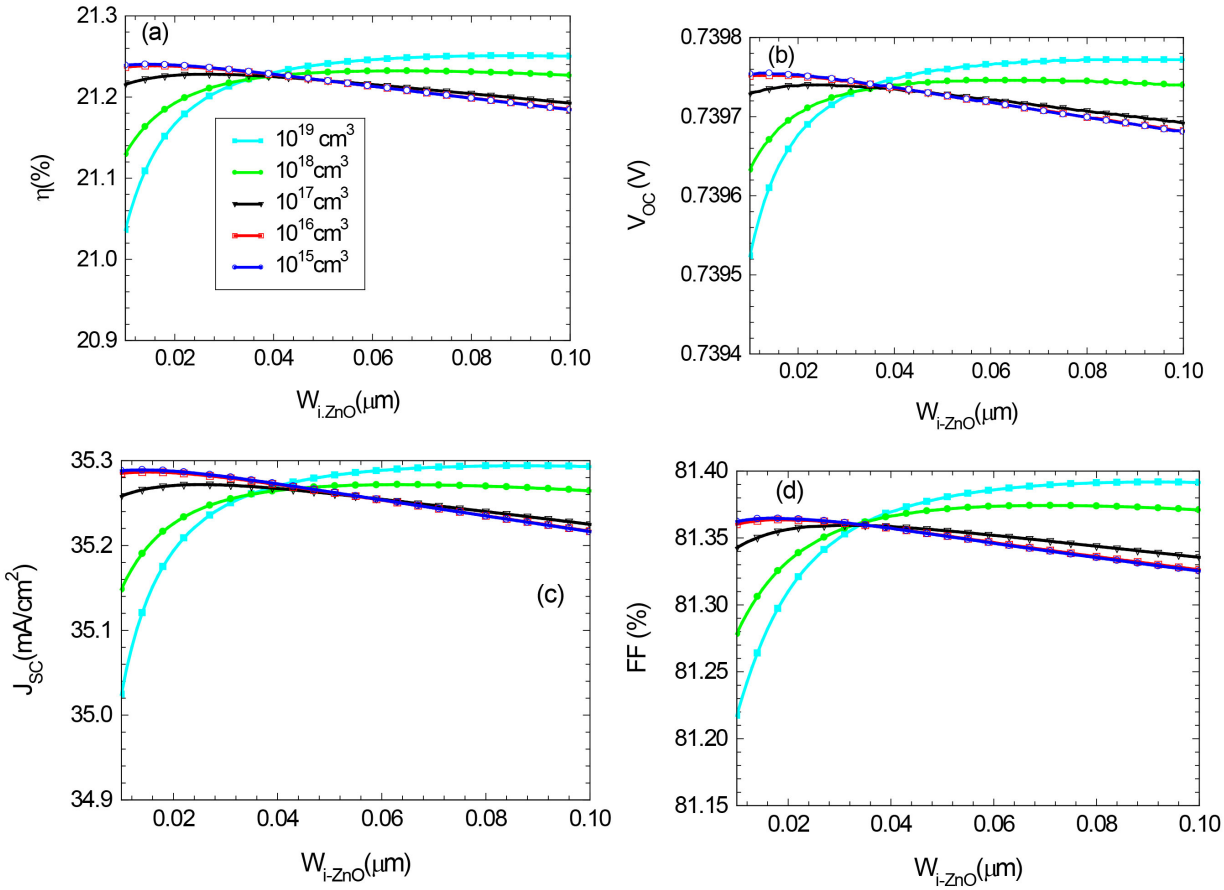


**Figure 7.** Variation of electrical parameters as a function of i-ZnO layer thickness for different dopant density values.

The results obtained are also represented by **Figure 8**. At low thickness of ZnO:Al the cell parameters improve with decreasing doping densities, The best cell performances are obtained for à thin layer of ZnO:Al (0.015 μm to 0.06 μm) with efficiency around 21.16% for dopant densities between $10^{15}$ cm$^{-3}$ and $10^{16}$ cm$^{-3}$.

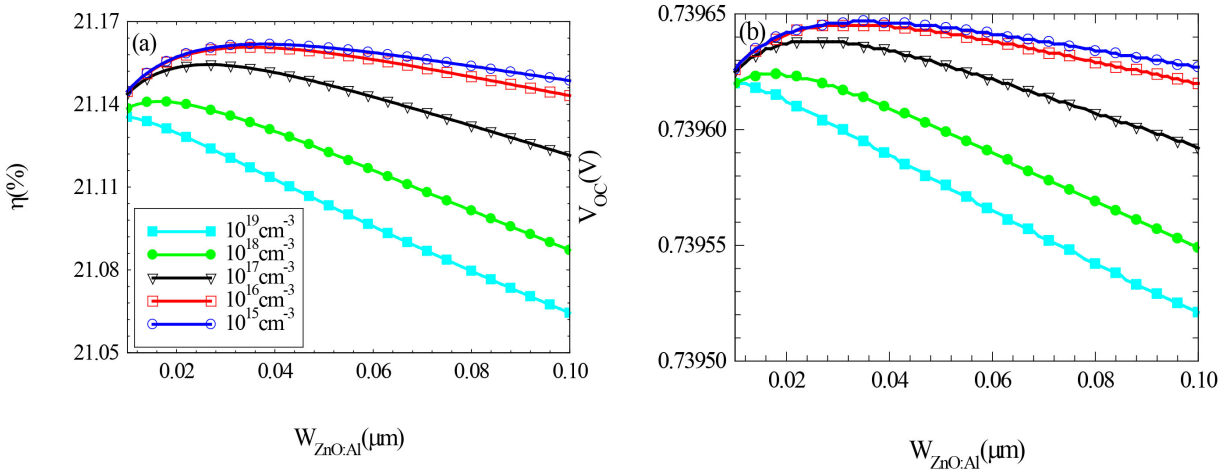

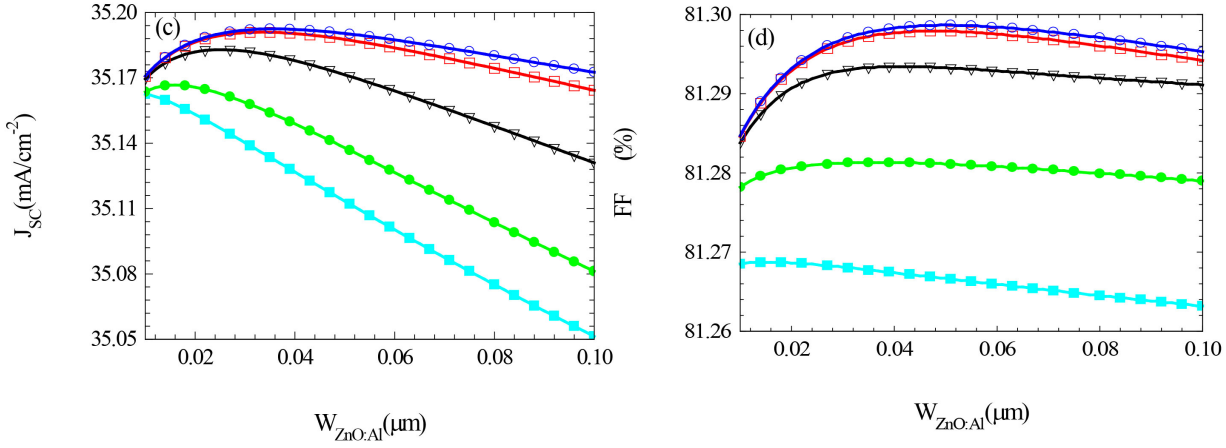


**Figure 8.** Variation of electrical parameters as a function of ZnO: Al layer thickness for different dopant density.

For doping densities higher than $10^{17}$ cm$^{-3}$, the cell is no longer efficient. Optimal doping significantly reduces electrical resistivity and increases conductivity, thus facilitating the collect of photogenerated charge carriers. On account of too high density can introduce crystalline defect or volume imperfections. The right choice ZnO:Al thickness allows visible light to be effectively exploited.

Optimizing the performance of CIGS-based photovoltaic cells requires understanding the mechanisms of i-ZnO/CdS junction formation. The formation of the junction between I-ZnO and CdS involves chemical interaction phenomena that depend, on the hand, on the geometry of the layers and, on the other hand, on the initial deposition [22] [23]. Interface states strongly influence the band diagram and distort layer contact. These interface states are located on discrete levels of the semiconductor's bandgap, and can by caused by the abrupt breakdown of the crystal lattice at the semiconductor surface.

### 3.3. Influence of the Conduction Band Offset at the ZnO/CdS Interface

Before reaching the CIGS layer, solar radiation must pass through the ZnO layer, which must be both transparent and conductive. The deposition of the ZnO layer requires high energy, which can have a direct impact on the overall performance of the solar cell. Several studies have shown that the ZnO/CdS interface acts as a recombination center for photo-generated charge carriers in the absorber [17] [18].

Building on this, we will investigate the influence of the conduction band offset at this interface, as it plays a key role in charge carrier recombination**.** The band offset is determined from the electronic affinities of the ZnO and CdS layers, and the equations at band level are given according to the Minemoto model [24] Equation (6) and Equation (7).

For the conduction band.

$$\Delta Ec = q\left(\chi_{CdS} - \chi_{ZnO}\right) \tag{6}$$

And for valence band offset

$$\Delta Ev = Eg(\mathrm{ZnO}) - Eg(\mathrm{CdS}) - \Delta Ec \quad (7)$$

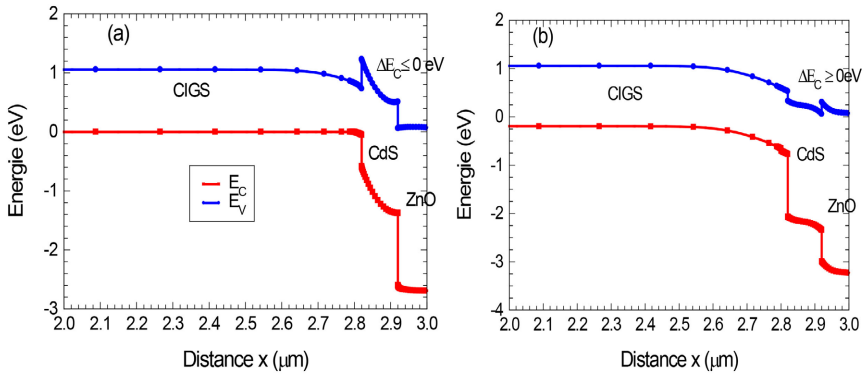


**Figure 9.** Energy band diagram of conduction band at the ZnO/CdS interface showing (CBO) cliff (a) and peak (b).

The conduction band offset (CBO) at the ZnO/CdS interface, as shown in **Figure 9**, can form either a cliff or a spike. A cliff occurs when, $\chi_{CdS} < \chi_{ZnO}$ **Figure 9(a)** which constitutes a barrier to current flow in the cell. Conversely, a spike appears, when $\chi_{CdS} > \chi_{ZnO}$ **Figure 9(b)**. This spike tends to lower the potential barrier across the cell which increases the recombination rate at the ZnO/CdS interface. **Figure 10** shows the evolution of electrical parameters as a function of conduction band between Cd Sans ZnO. A deep cliff (CBO < −0.45 eV) at the ZnO/CdS interface hinders efficient electron collection.

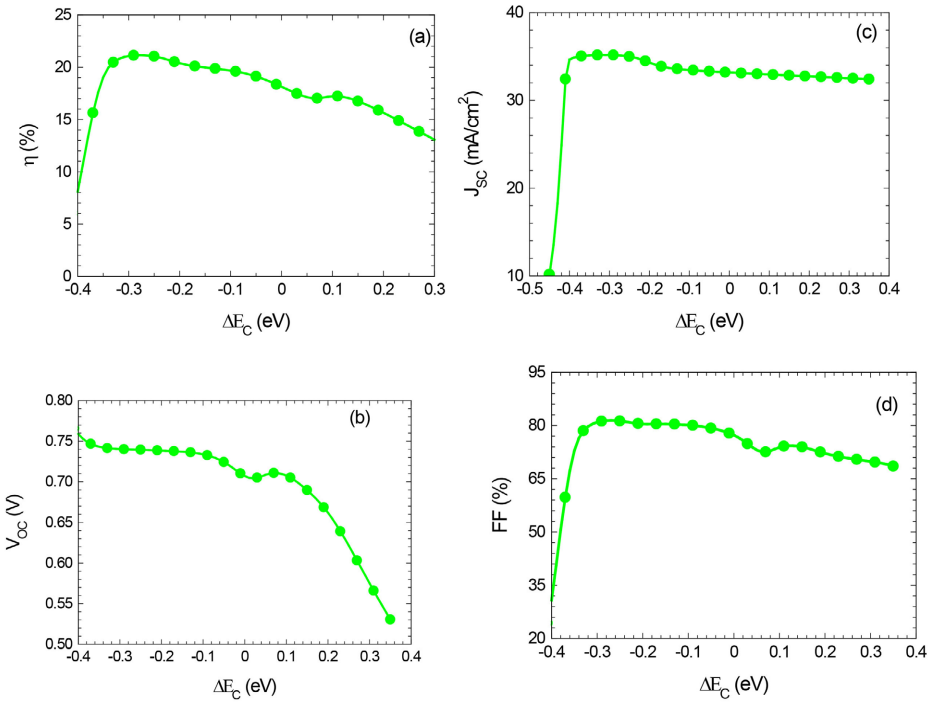


**Figure 10.** Variation of electrical parameters as a function of conduction band offset at the ZnO/CdS interface.

However, the cliff is less pronounced (CBO ≈ −0.3 eV), electrons are collected more successfully, leading to higher efficiency, open short-circuit current and fell factor. In this case, the electrons can overcome the potential barrier, enhancing the overall performances of the solar cell.

## 4. Conclusion

The performance of a CIGS solar cell in generating electron-hole pairs depends on the number of photons absorbed. In this work, we have evaluated the losses caused by defects in the ZnO layer and defects of i-ZnO/n-CdS interface, with allowed us to identify optimal parameters values for the efficient operation of the CIGS solar cell. Simulation using the SCAPS software shows that for good exploitation of the solar spectrum, the thickness of the ZnO window layer must be around $W_{\text{i-ZnO}} = 0.02$ µm and $W_{\text{ZnO:Al}} = 0.035$ µm to allow high transparency to incident radiation. The aluminum content is estimated at 8%, corresponding to a doping concentration of approximately $10^{15}$ $cm^{-3}$, which provides a suitable band-gap for good transparency of the ZnO layer. To reduce recombination at the n-CdS/i-ZnO interface, the electron affinity of ZnO should be greater than that of CdS, with the optimal value corresponding to a conduction band offset of approximately −0.3 eV.

## Conflicts of Interest

The authors declare no conflicts of interest regarding the publication of this paper.

## References

[1] Jackson, P., Wuerz, R., Hariskos, D., Lotter, E., Witte, W. and Powalla, M. (2016) Effects of Heavy Alkali Elements in Cu(In,Ga)$Se_2$ Solar Cells with Efficiencies up to 22.6%. *Physica Status Solidi—Rapid Research Letters*, **10**, 583-586. https://doi.org/10.1002/pssr.201600199

[2] Powalla, M., Jackson, P., Witte, W., Hariskos, D., Paetel, S., Tschamber, C., *et al.* (2013) High-Efficiency Cu(In,Ga)$Se_2$ Cells and Modules. *Solar Energy Materials and Solar Cells*, **119**, 51-58. https://doi.org/10.1016/j.solmat.2013.05.002

[3] Nichiporuk, O., Kaminski, A., Skryshevsky, V. and Litvinenko, S. (2005) Mis-Stimulated Back-Surface Passivation of Interdigitated Back-Contacts Solar Cells. *Solar Energy Materials and Solar Cells*, **87**, 549-555. https://doi.org/10.1016/j.solmat.2004.08.018

[4] Ruckh, M., Schmid, D. and Schock, H.W. (1994) Photoemission Studies of the ZnO/CdS Interface. *Journal of Applied Physics*, **76**, 5945-5948. https://doi.org/10.1063/1.358417

[5] Burgelman, M., Verschraegen, J., Degrave, S. and Nollet, P. (2004) Modeling Thin-Film PV Devices. *Progress in Photovoltaics*: *Research and Applications*, **12**, 143-153. https://doi.org/10.1002/pip.524

[6] Islam, M.M., Ishizuka, S., Yamada, A., Matsubara, K., Niki, S., Sakurai, T., *et al.* (2011) Thickness Study of Al: ZnO Film for Application as a Window Layer in Cu(In1-xGax)$Se_2$ Thin Film Solar Cell. *Applied Surface Science*, **257**, 4026-4030. https://doi.org/10.1016/j.apsusc.2010.11.169

[7] Yilbas, B.S., Keles, O. and Toprakli, A.Y. (2017) Surface Engineering Towards Self-

Cleaning Applications: Laser Textured Silicon Surface. *Procedia Engineering*, **184**, 716-724. https://doi.org/10.1016/j.proeng.2017.04.147

[8] Ashida, N., Murata, M., Hironiwa, D., Chantana, J., Uegaki, H. and Minemoto, T. (2015) Numerical Analysis of Cu(In,Ga)$Se_2$ Solar Cells with High Defect Density Layer at Back Side of Absorber. *Physica Status Solidi C*, **12**, 638-642. https://doi.org/10.1002/pssc.201400242

[9] Kim, K., Gwak, J., Ahn, S.K., Eo, Y., Park, J.H., Cho, J., *et al.* (2017) Simulations of Chalcopyrite/c-Si Tandem Cells Using SCAPS-1D. *Solar Energy*, **145**, 52-58. https://doi.org/10.1016/j.solener.2017.01.031.

[10] Uddin, M.S., Hosen, R., Sikder, S., Mamur, H. and Bhuiyan, M.R.A. (2024) Photovoltaic Performance Enhancement of Al/ZnO: Al/i-ZnO/CdS/CIGS/Pt Solar Cell Using SCAPS-1D Software. *Next Energy*, **2**, Article 100080. https://doi.org/10.1016/j.nxener.2023.100080

[11] Ouédraogo, S., Zougmoré, F. and Ndjaka, J.M.B. (2014) Computational Analysis of the Effect of the Surface Defect Layer (SDL) Properties on Cu(In,Ga)$Se_2$-Based Solar Cell Performances. *Journal of Physics and Chemistry of Solids*, **75**, 688-695. https://doi.org/10.1016/j.jpcs.2014.01.010

[12] Traoré, B., Ouédraogo, S., Kébré, M.B., Oubda, D., Sankara, I., Zongo, A., *et al.* (2023) Effect of Defects at the Buffer Layer CdS/absorber CIGS Interface on CIGS Solar Cell Performance. *Advances in Chemical Engineering and Science*, **13**, 289-300. https://doi.org/10.4236/aces.2023.134020

[13] Ouédraogo, S. (2016) Modélisation numérique d'une cellule solaire à couches minces à base de CIGS.

[14] Trenque, I. (2024) Synthèse et caractérisation d'oxydes métalliques ZnO au bénéfice de nouvelles stratégies d'élaboration d'absorbeurs IR.

[15] Guirdjebaye, N., Ouédraogo, S., Teyou Ngoupo, A., Mbopda Tcheum, G.L. and Ndjaka, J.M.B. (2019) Junction Configurations and Their Impacts on Cu(In,Ga)$Se_2$ Based Solar Cells Performances. *Opto-Electronics Review*, **27**, 70-78. https://doi.org/10.1016/j.opelre.2019.02.001

[16] Gloeckler, M., Sites, J.R. and Metzger, W.K. (2005) Grain-Boundary Recombination in Cu(In,Ga)$Se_2$ Solar Cells. *Journal of Applied Physics*, **98**, Article 113704. https://doi.org/10.1063/1.2133906

[17] Stjerna, B., Granqvist, C.G., Seidel, A. and Häggström, L. (1990) Characterization of Rf-Sputtered $SnO_x$ Thin Films by Electron Microscopy, Hall-Effect Measurement, and Mössbauer Spectrometry. *Journal of Applied Physics*, **68**, 6241-6245. https://doi.org/10.1063/1.346889

[18] Duenow, J.N., Gessert, T.A., Wood, D.M., Egaas, B., Noufi, R. and Coutts, T.J. (2008) Zno:al Doping Level and Hydrogen Growth Ambient Effects on CIGS Solar Cell Performance. 2008 33*rd IEEE Photovolatic Specialists Conference*, San Diego, 11-16 May 2008, 1-5. https://doi.org/10.1109/pvsc.2008.4922533

[19] Abdelkader, H., Fayssal, Y., Warda, D., Nadhir, A. and Salah, A.M. (2011) Les propriétés structurales, optiques et électriques des couches minces de ZnO: Al élaborées par spray ultrasonique.

[20] Naghavi, N., Abou-Ras, D., Allsop, N., Barreau, N., Bücheler, S., *et al.* (2010) Buffer Layers and Transparent Conducting Oxides for Chalcopyrite Cu(In,Ga)(S,$Se)_2$ Based Thin Film Photovoltaics: Present Status and Current Developments. *Progress in Photovoltaics: Research and Applications*, **18**, 411-433. https://doi.org/10.1002/pip.955

[21] Ma, A. (2015) Étude et optimisation d'un procédé plasma basse puissance pour le dépôt de ZnO dopé et non dopé à propriétés photovoltaïques à partir d'une solution

aqueuse.

[22] Guillemin, S. (2014) Mécanismes de croissance de nanostructures de ZnO par voie chimie liquide et caractérisation avancée.

[23] Slimi, H. (2019) Elaboration et caractérisation de couches minces co-dopées In, Co, préparées par la pulvérisation cathodique, applications aux cellules photovoltaïques.

[24] Minemoto, T., Okamoto, A. and Takakura, H. (2011) Sputtered ZnO-Based Buffer Layer for Band Offset Control in Cu(In,Ga)$Se_2$ Solar Cells. *Thin Solid Films*, **519**, 7568-7571.